ELSEVIER

Journal of Chromatography A, 734 (1996) 75–81

JOURNAL OF CHROMATOGRAPHY A

Profiles of large-size system peaks and vacancy bands in liquid chromatography
II. Comparison of experimental and calculated profiles

Peter Sajonz[a], Tong Yun[a], Guoming Zhong[a], Torgny Fornstedt[a], Georges Guiochon[a,b,*]

[a] *Department of Chemistry, University of Tennessee, Knoxville, TN 37996-1600, USA*

[b] *Division of Analytical Chemistry, Oak Ridge National Laboratory, Oak Ridge, TN 37831-6120, USA*

Abstract

The profiles of large-size system peaks and vacancies have been studied and compared. A reversed-phase system was used with an analytical-size column packed with ZORBAX C_{18} spherical particles and methanol–water as the mobile phase. The analyte was 3-phenyl-1-propanol. The equilibrium–dispersive model of chromatography was used to calculate band profiles using the measured isotherm data and the column efficiency. The isotherm data were determined using frontal analysis and could be fitted to a simple Langmuir equation. Excellent agreement was found between experimental and calculated results.

Keywords: System peaks; Vacancy bands; Preparative chromatography; Band profiles

1. Introduction

System peaks and vacancies are observed when an injection is made in a chromatographic column previously equilibrated with a mobile phase consisting of a solution with a constant concentration of an additive which participates in the retention mechanism [1]. Upon injection of a large sample containing dilute analytes, an important perturbation in the concentration of the additive occurs which propagates during the elution of the mixture. Depending on the relative concentration of the additive in the mobile phase and in the sample, this perturbation can be a system peak or a vacancy. System peaks correspond to the injection of a volume of sample in which the additive concentration is higher than the plateau concentration, hence, to the injection of a net excess of this component. Vacancies are obtained when the additive concentration in the sample is lower than the plateau concentration. They can be considered as the injection of a negative amount of the component. Because the additive concentration influences considerably the retention of the analytes, interferences occur between the analyte peaks and the additive band the profile of which tends to act as a concentration gradient. It is important to investigate the (positive or negative) concentration profile of the additive band to better understand this phenomenon which has proven useful in clinical and other biochemical analyses [2]. The companion paper [3] reviews the present state of the art in the study of system peaks and describes the analytical solution of the ideal of chromatographic model for the initial and boundary conditions corresponding to this problem.

The ideal model assumes that the column efficiency is infinite. All actual columns have a finite

*Corresponding author. Address for correspondence: Department of Chemistry, University of Tennessee, Knoxville, TN 37996-1600, USA.

0021-9673/96/$15.00
SSDI 0021-9673(95)00982-5

efficiency. Actual band profiles can be derived from more complex models which take into account the influence of this finite efficiency [1]. In most practical cases encountered in HPLC, excellent agreement is obtained between experimental band profiles and the profiles calculated as solutions of the equilibrium–dispersive model [1]. It has been shown, however, that the band profiles calculated with this model are in reasonable agreement with the experimental results only if the column efficiency is high and the amount of sample injected is large. More precisely, this agreement is very good if the dimensionless number $m = NL_f[k'_0/(1 + k'_0)]^2$ is larger than 35 [4]. The goal of this paper is to compare experimental results with the numerical solution of the equilibrium–dispersive model and with the analytical solution of the ideal model.

2. Theory

The solution of the ideal model for the profiles of large-size system peaks and vacancies under nonlinear conditions has been presented in the companion paper [3]. System peaks have a Langmuirian profile with a front shock boundary and a rear diffuse boundary. The profiles of the system peaks are given by an equation which is very similar to the one giving the elution profile of high-concentration bands. The same equation gives the profile of the rear diffuse boundary in both cases. Because the velocity associated with a concentration decreases with decreasing concentration and the vacancy is a negative concentration fluctuation, vacancy peaks have an anti-Langmuirian profile, with a front diffuse boundary and a rear shock boundary. Again, the equations are very similar. The equation giving the profile of the diffuse boundary is the same as in the previous cases (elution and system peak), except for a translation of $-t_p$, the width of the rectangular pulse injected. This difference results from the different origins of the diffuse boundaries. In system peaks the rear shock of the injection is unstable while in vacancies it is the front shock of the injection which is unstable [3].

In the ideal model, the column efficiency is assumed to be infinite. In the differential mass balance of chromatography, the dispersion term is canceled and the stationary-phase concentration is related to the mobile-phase concentration by the isotherm equation, assuming constant equilibrium between the two phases [5]. In the equilibrium–dispersive model this latter condition is kept, but the dispersion term is not canceled. The apparent axial dispersion accounts for all band spreading phenomena, including axial diffusion, eddy diffusion, and mass-transfer resistances [5]. The correction is approximate but satisfactory in most cases if the column efficiency is high and the sample size large, so nonlinear effects are important [4,5]. This model has been discussed in detail and all relevant information can be found easily [5].

There are no analytical solutions of the equilibrium–dispersive model but the calculation of numerical solutions is now simple [5] and fast [6]. The finite difference method using the forward–backward scheme [5] has been used in this work.

3. Experimental

3.1. Equipment

An HP1090 liquid chromatographic system was used for all the experiments (Hewlett-Packard, Palo Alto, CA, USA). It is equipped with a multisolvent delivery system, an automatic sample injector, a column oven, a diode-array detector, and a data acquisition system.

3.2. Temperature control

All experiments were carried out at 35°C. For maximum temperature accuracy the column was placed in a water bath located right in front of the column oven of the HP1090. The eluent [water–methanol (60:40)] was preheated to 35°C. The heat exchanger was also set to 35°C, in order to avoid heat losses.

3.3. Column

A 15×0.46 cm column was used. It was packed with C_{18} silica (10 μm average particle size, 150 Å

average pore size) from ZORBAX (BTR, Wilmington, DE, USA), using a slurry technique with methanol as the pushing solvent and dichloromethane as the slurry solvent. The packing pressure was raised gradually to $4.5 \cdot 10^7$ Pa (6500 p.s.i.) and 200 ml of methanol were flushed through the column. The column was tested using samples from a 1% acetone solution in methanol and pure methanol as the mobile phase. An efficiency of 4800 theoretical plates calculated from the peak width at half-height was obtained at 1 ml/min, which was deemed satisfactory for the experiments reported here.

3.4. Materials

Methanol was HPLC grade (Baxter), water was deionized and filtered through a 0.2-μm cellulose acetate filter. 3-Phenyl-1-propanol (98% pure) was purchased from Fluka and filtered through a 0.45-μm Nylon filter (Nalgene Filterware NYL 153-0045, Nalgene, NY, USA). All chemicals were degassed by sonication before use.

3.5. Isotherm determination

The equilibrium isotherm of 3-phenyl-1-propanol was determined using the staircase frontal analysis method. A sample solution containing 30 mg/ml of 3-phenyl-1-propanol in the mobile phase (solvent A) was prepared and used as solvent B in the solvent delivery system. The steps were made using the solvent delivery system of the chromatograph, the precision and accuracy of which have been demonstrated previously [7].

3.6. Isotherm Calculation

The amount adsorbed for each successive step was obtained using the following equation:

$$q_{i+1} = q_i + \frac{C_{i+1} - C_i}{F} \frac{t_{R,i+1} - t_0}{t_0}$$

where F is the phase ratio [3], $t_{R,i+1}$ the retention time of the breakthrough curves obtained from the retention time of its half-height, t_0 the hold-up time of the column, q_i the stationary phase concentration of the component in equilibrium with the mobile phase concentration C_i, i being the step rank. The column hold-up time was taken as the retention time of uracil, assumed to be non-retained with this mobile phase. From the value of t_0, the column porosity and the phase ratio were derived and found to be $\varepsilon_T = 0.585$ and $F = 0.709$.

The isotherm data are shown in Fig. 1. They could be fitted to a simple Langmuir equation [$q = aC/(1 + bC)$] with a very small residual. A nonlinear regression method was used, which minimized the squares of the relative differences between the experimental and calculated values of q [8]. The numerical values of the coefficients of the Langmuir isotherm were $a = 9.25$ and $b = 0.0621$ ml/mg.

3.7. Chromatograms

The band profiles were recorded at 265 nm. Three different injection volumes were chosen (200, 100, and 50 μl) and four different concentrations (0, 5, 15, and 20 mg/ml). The mobile phase was methanol–water (40:60) containing 10 mg/ml of 3-phenyl-1-propanol. The flow-rate used was 1 ml/min in all experiments.

Calibration of the detector was carried out using the concentration plateaus acquired during the frontal analysis experiments. The calibration data were not linear but could be fitted to a third-order polynomial

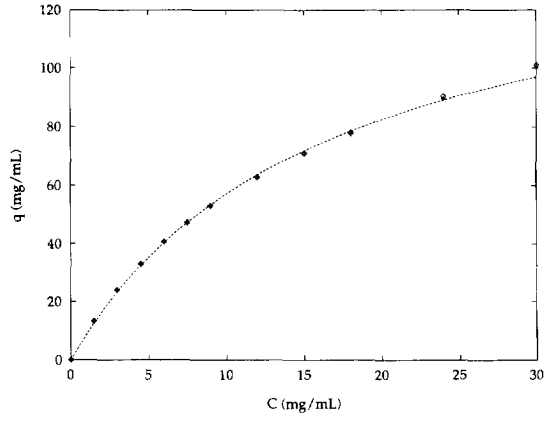

Fig. 1. Isotherm data (symbols) with best Langmuir fit (line).

equation. Some of the differences between calculated and experimental band profiles can be due to errors in the calibration curve or to a drift of its parameters.

The column efficiency was measured by injecting 10-μl samples of pure mobile phase methanol–water (40:60) on the concentration plateau of 3-phenyl-1-propanol at 10 mg/ml. The efficiency of the negative peak was derived from its width at half-height and was found to be 3120 theoretical plates.

4. Results and discussion

Chromatograms of system peaks and vacancies were calculated using the equilibrium–dispersive model with the experimental conditions under which the experiments reported in this work were carried out, except for the column efficiency. These calculations were made for efficiencies of 1000, 3000 and 10 000 theoretical plates. The bands obtained are shown in Fig. 2 and compared to the profiles predicted by the ideal model, profiles which were calculated using the equations derived in Ref. [3]. There is not much difference between the last profile, at 10 000 plates, and the profile corresponding to an infinite column efficiency. The shock has been dispersed into a steep shock layer and the diffuse boundaries have been made smoother. Instead of ending at a finite time, as the solutions of the first-order hyperbolic partial differential equation (Eq. 1, Ref. [3]), the solution has the abscissa axis as an asymptote, because the mass balance of chromatography becomes a parabolic equation when the dispersion term is included [5]. This dispersive effect tends to make the profiles of a pulse and a vacancy of the same magnitude more alike than they are for mere thermodynamic reasons.

Fig. 3a–d show a comparison between the elution profiles of a very large pulse (no additive in the weak solvent, $C_a=0$), system peaks (additive at $C_a=10$ mg/ml in the weak solvent, $C_{inj}>C_a$), and vacancies ($C_a=10$ mg/ml, $C_{inj}<C_a$) calculated with different values of the column efficiency. All profiles correspond to the same injection volume (200 μl), hence to the same value of the injection time t_p (i.e., 0.2 min). However, in all four figures, the elution profiles of the elution peak and the system peak have been moved backward by an amount equal to t_p,

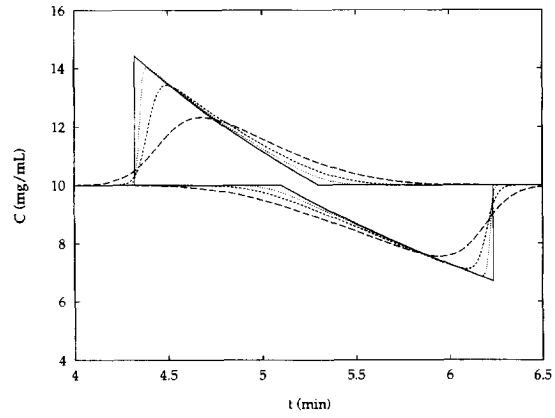

Fig. 2. Chromatograms calculated with the ideal and the equilibrium–dispersive models for a large pulse of an additive (system peak) and for a vacancy of the same amount, both eluted by a mobile phase containing the additive at a concentration $C_a=10$ mg/ml. Concentrations in the injected samples: $C_{inj}=20$ mg/ml (pulse) or $C_{inj}=0$ (vacancy). Duration of the injection $t_p=0.2$ min. Column length, 10 cm. Column efficiency, solid line, infinite; dotted line, 10 000 plates; dashed line, 3000 plates; longdashed line, 1000 plates.

which explains the difference between these figures and Fig. 2. As shown previously [3], this should bring all diffuse boundaries to coincide. For the ideal model (infinite column efficiency, Fig. 3a) the diffuse rear of the large elution profile ($C_a=0$) overlays exactly with the diffuse rear of the system peak and the diffuse front of the vacancy. All three chromatograms have one common point at $t=5.1$ min and $C_a=10$ mg/ml. Decreasing the column efficiency to 10 000 (Fig. 3b), 3000 (Fig. 3c), and 1000 (Fig. 3d) has almost no effect on the profile of the elution band. This is essentially due to the strong degree of overloading of the column. In contrast, the features of the system peak and vacancy are considerably eroded when the efficiency decreases. Below 3000 plates, these profiles have nothing in common with those predicted by the ideal model and cannot be used for thermodynamic determinations. These injections are merely moderate perturbations of the baseline.

Fig. 4 illustrates the influence of the injection volume on the size of the system peak and vacancy obtained. In all these figures a time-scale shift has been made for the positive peaks (as explained above for Fig. 3a–d). Three sample volumes – increasing

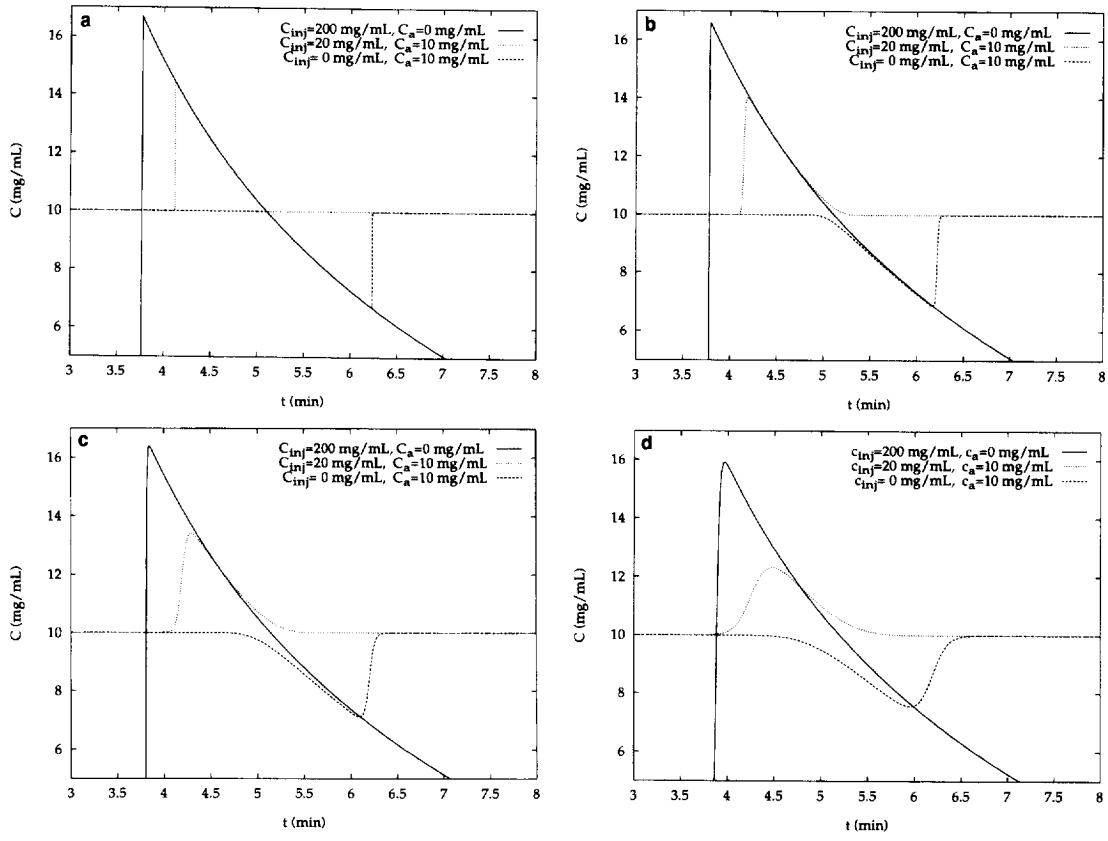

Fig. 3. Illustration of the influence of the column efficiency on the elution profile, the system peak and the vacancy. The time scale has been shifted by t_p=0.2 min for the elution profile and system peak, to bring the diffuse parts of these profiles and of the vacancy profile into coincidence. (a) $N=\infty$, (b) N=10 000, (c) N=3000, (d) N=1000.

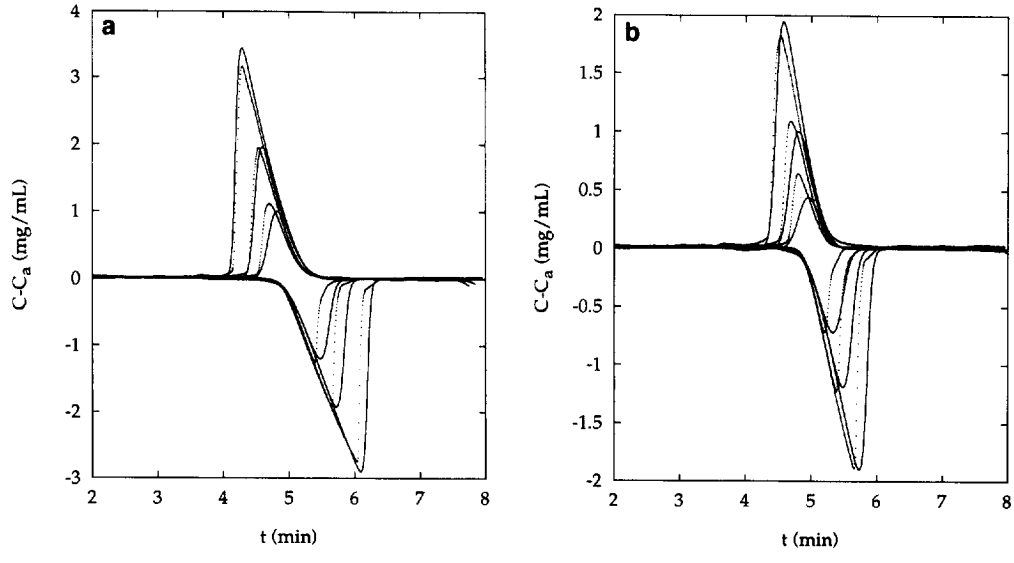

Fig. 4. Experimental and simulated band profiles for different injection volumes. The injection time is subtracted for the positive peaks. C_a=10 mg/ml. (a) C_{inj}=0, 20 mg/ml, V_{inj}=200, 100, and 50 μl; (b) C_{inj}=5, 15 mg/ml

in geometric progression have been used – 50, 100, and 200 μl (i.e., t_p=0.05, 0.1, and 0.2 min). The solutions used for the positive pulses had concentrations of 20 and 15 mg/ml, respectively for Fig. 4a and 4b. The solutions used for the vacancies had concentrations of 0 and 5 mg/ml, respectively. In both cases, each pulse corresponds to a vacancy of the same absolute size, and hence the same area. The experimental profiles are in excellent agreement with the calculated ones, especially for the largest amounts injected, in which case the nonlinear effects are the most intense. Note that the highest concentrations achieved, at the top of the largest pulses are below 14 mg/ml, corresponding to a region where the isotherm data fit very well to the Langmuir model. The diffuse boundaries of all three ex-

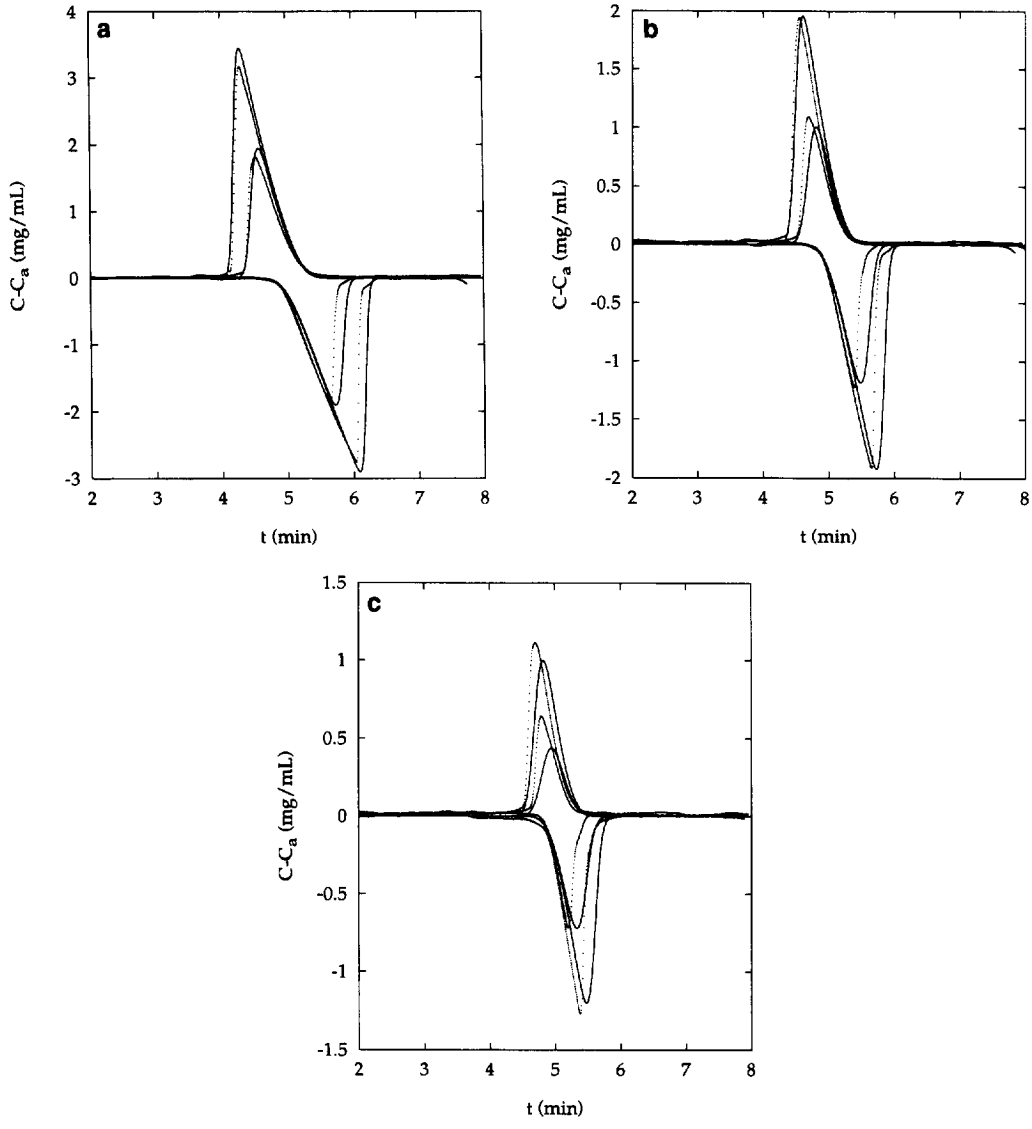

Fig. 5. Experimental and simulated band profiles for different injection concentrations. The injection time is subtracted for the positive peaks. (a) V_{inj}=200 μl, C_{inj}=0 and 20 mg/ml, C_a=10 mg/ml; (b) V_{inj}=100 μl; (c) V_{inj}=50 μl.

perimental peaks are overlaid with great exactitude, although they are slightly different from those predicted by the model. As just explained, this cannot be caused by an error on the isotherm. It is plausible that the slight differences observed are caused by the use of an apparent axial dispersion coefficient which is independent of the concentration whereas there is increasing evidence that this assumption is often not correct [9].

In Fig. 5a–c, the same data are compared to illustrate the influence of the sample concentration at constant volume injected. The agreement between experimental and calculated profiles is excellent in Fig. 5a and 5b, which corresponds to the larger bands. It is less satisfactory in Fig. 5c, which corresponds to the smallest fluctuation made. Even in this case, the difference between the calculated and observed values of the retention time is of the order of 3%, not a very large error.

5. Conclusion

This work confirms that very accurate predictions of band profiles can be made in nonlinear chromatography, provided that the equilibrium isotherm and the column efficiency are measured with accuracy and precision. While precision is nowadays easy to achieve when high-quality instruments are used, accuracy may be a more difficult issue. The quality of the agreement observed and reported in Fig. 4 and Fig. 5 is for a large part due to the use of an efficient column, of a highly stable and reliable instrument, and of a precise temperature control. Operation of the column at constant temperature was critical for the success of this work.

Acknowledgments

This work has been supported in part by Grant CHE-9201663 of the National Science Foundation and by the cooperative agreement between the University of Tennessee and the Oak Ridge National Laboratory. We acknowledge the support of our computational effort by the University of Tennessee Computing Center. We are grateful to Klaus Lohse (BTR, Wilmington, DE, USA) for the gift of the packing material. TF is grateful for the financial support awarded to him by Astra Hässle AB (Mölndal, Sweden) and by the Swedish Academy of Pharmaceutical Sciences (The Göran Schill Memorial Foundation).

References

[1] G. Guiochon, S. Golshan Shirazi and A.M. Katti, Fundamentals of Preparative and Nonlinear Chromatography, Academic Press, Boston, MA, 1995, Ch. XIII.

[2] T. Fornstedt, D. Westerlund and A. Sokolowski, J. Liq. Chromatogr., 11 (1988) 2645.

[3] G. Zhong, T. Fornstedt and G. Guiochon, J. Chromatogr. A, 734 (1996) 63.

[4] B.C. Lin, T. Yun, G. Zhong and G. Guiochon, J. Chromatogr. A, 708 (1995) 1.

[5] G. Guiochon, S. Golshan Shirazi and A.M. Katti, Fundamentals of Preparative and Nonlinear Chromatography, Academic Press, Boston, MA, 1995, Ch. X.

[6] A. Felinger and G. Guiochon, J. Chromatogr. A, 658 (1994) 511.

[7] M.Z. El Fallah and G. Guiochon, Anal. Chem., 63 (1991) 859.

[8] G. Guiochon, S. Golshan Shirazi and A.M. Katti, Fundamentals of Preparative and Nonlinear Chromatography, Academic Press, Boston, MA, 1995, Ch. III.

[9] H. Guan, P. Sajonz, G. Zhong and G. Guiochon, Biotechnol. Progress., submitted for publication.